3D RESAMPLING FOR AIRBORNE LASER DATA OF URBAN AREAS

S. Zinger, M. Nikolova, M. Roux, H. Maître

Ecole Nationale Supérieure des Télécommunications
46 rue Barrault, 75634 Paris Cedex 13, France
zinger@tsi.enst.fr, nikolova@tsi.enst.fr, mroux@tsi.enst.fr, henri.maitre@enst.fr

KEY WORDS: laser scanning, urban areas, irregular sampling, DEM

ABSTRACT

We consider the problem of resampling for the data obtained by laser scanning on an irregular grid. The data obtained by airborne laser scanning are scattered, and the resampling on a regular grid is needed for the generation of digital surface models (DSM). Some well-known methods are considered in this article: triangle-based linear interpolation, triangle-based nearest neighbor interpolation and kriging. An energy minimization approach is proposed which allows to avoid the drawbacks relevant to these methods. This approach allows to impose a model of surface corresponding to urban areas. The energy function is adapted to deal with the scattered data, and its parameters are chosen to fit the model of a urban area. A correlation coefficient is used to compare the results. The methods are tested on real data - irregularly spaced 3D points - laser scanner data of Brussels. Visual and numerical experimentation results are presented.

1 INTRODUCTION

Laser scanning allows to measure the height of the terrain from an aircraft sending a pulse towards the ground and measuring the time for the reflected pulse to come back. As an output it gives coordinates of 3D points of the terrain. We will consider the data representing urban areas. Due to the acquisition technique, these points are irregularly spaced while one needs to have them on a regular grid for most of possible applications. In this paper we consider methods of 3D resampling applied for urban areas. Images of urban areas are characterized by homogeneous zones (roofs, streets), separated by edges. In an altimetric image height values are represented by gray level values. Let us emphasize that edges contain critical information, especially for urban images, since they delimit streets and buildings.

Classical approaches for the resampling of laser data on a regular grid are nearest neighbour and linear interpolation. In (Behan, 2000), both approaches are tested and evaluated with regards to the grid size and the DSM quantization towards the problem of overlapping strips matching. The grid size is recommended to be very similar to the original density of the data, the better results are reached with linear interpolation. Statistical interpolation methods, like kriging and linear prediction, are also proposed for the resampling over non-urban areas (Lohmann et al., 1999). The main drawback of these different approaches is either to oversmooth or to deform the building edges.

The suitable approach is supposed to give horizontal or oblique surfaces, i.e. roofs of buildings, and strong discontinuities, i.e. differences between roofs and ground, which are usually presented by straight lines, because of the form of facades. In order to cope with this problem we define the sought image to be a minimizer of a regularized cost function. We describe this approach and its implementation. Then we make experiments to determine the performance. We check the relevance of our results comparing with the altimetric data obtained from the optical images.

2 SOME RESULTS OF CLASSICAL APPROACHES

The classical methods for scattered data interpolation are triangle-based linear interpolation, triangle-based nearest neighbour interpolation (Watson, 1992) and kriging (Noel, 1991). Triangle-based linear interpolation gives results which have problems with edges and represents facades with non-vertical surfaces (Figure 1).

Figure 1: Result of linear interpolation based on the Delaunay triangulation of the initial data (city of Brussels, ©Eurosense).

The drawback of triangle-based nearest neighbour interpolation is that the surface is very rough, i.e. there are no slopes, and changes between groups of values are very steep. Then oblique surfaces like some roof facets are represented with discontinous surface (Figure 2).

Kriging gives smooth areas, where edges are blurred (Figure 3). For this approach the spatial dependencies are expressed by the variogram (Noel, 1991), which has three parameters to be fit according to the data.

The aerial image of the area we are working on is shown on Figure 4. Its resolution is 8 cm per pixel.
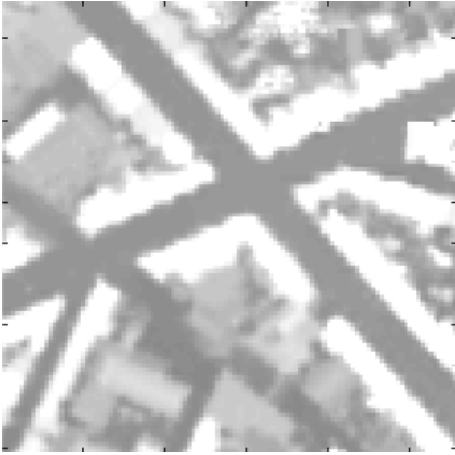
Figure 2: Result of nearest neighbour interpolation.

Figure 3: Result of kriging with a spherical model of variogram.

Figure 4: Aerial image of the studied area of Brussels (©Eurosense).

3 ENERGY MINIMIZATION APPROACH

One method for image restoration with edge preserving is based on energy minimization (Geman et al., 1992). In this approach a solution is an image which minimizes a cost function, also called energy. An expression for the energy consists of two terms:

- data-fidelity term, which penalizes variations between a surface and experimentally measured data

- regularization term, which imposes a *roughness penalty*.

The optimization of the energy is, in the general case, too expensive. One generally chooses to introduce a markovianity assumption which makes possible to ensure that a minimum can be obtained as a sum of local terms (this seems reasonable in our case, since it is probable that the quality of reconstruction of a roof of a building does not concern the geometry of other distant buildings). During the reconstruction, one makes iterative calculations of the surface so that a minimum of an energy is obtained. Several elements are significant for the method: the definition of the neighbourhood considered around each point, the definition of the terms of energy and the corresponding potentials, and, finally, a method to decrease an energy.

3.1 Definition of neighbourhood

Let observed data samples be $\{z(x_k, y_k)\}$ at positions (x_k, y_k) for $k = 1, ..., N$. We are looking for samples $u(i, j)$ on a regular grid (i, j).

The neighbourhood for the regularization term consists of points inside a circle, which includes 8 nearest points on the regular grid (Figure 5).
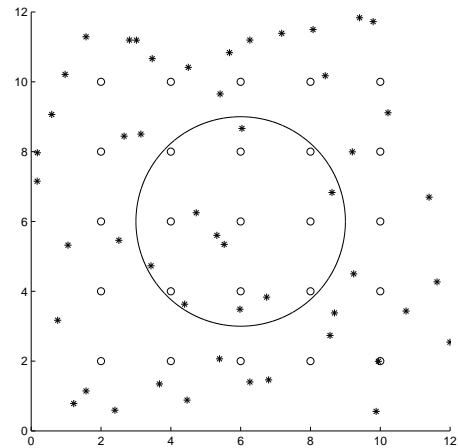

Figure 5: Definition of the neighbourhood of a pixel: it is represented by all the points located inside the circle. The stars represent the irregularly distributed original data, the circles are the regular points which one wants to determine.

So the neighbourhood for the regularization term for each point (i,j) is:

$$M(i, j) = \{(i', j') : dist((i', j'), (i, j)) \leq r\}$$

$$dist((x,y),(i,j)) = \sqrt{(x-i)^2 + (y-i)^2}$$

The radius r is chosen to encompass to the 8 nearest neighbours on a regular grid.

The neighbourhood for the data-term is:

$$P(i,j) = \{(x_k, y_k) : dist((x_k, y_k),(i,j)) \leq r\}$$

Thus for every position (i,j) we obtain a set of indexes of data points, say $K(i,j)$, which are placed in the neighbourhood of (i,j):

$$K(i,j) = \{k : (x_k, y_k) \in P(i,j)\}$$

3.2 Expression for the cost function

The form of the energy generally consists of 2 terms, data-fidelity term and regularization-term. For our problem, we have chosen the following cost function:

$$F(u) = \sum_{i,j} \left(\begin{array}{c} \sum_{K(i,j)} \psi \left(\frac{z(x_k,y_k)-u(i,j)}{\text{dist}((x_k,y_k),(i,j))} \right) \\ + \alpha \sum_{M(i,j)} \varphi \left(\frac{u(i',j')-u(i,j)}{\text{dist}((i',j'),(i,j))} \right) \end{array} \right) \tag{1}$$

where ψ and φ are potential functions, and the multiplier α gives a weight to the regularization term. The first summation (on i and j) will be made on all the points of the regular grid. The second summation (on the set K) is done on all the points of the irregular grid inside the circle of neighbourhood of the current point i,j. The third summation is done on the 8 neighbors of the current point i,j. The solution $\hat{u}$ will be a surface which minimizes the cost function:

$$\hat{u} = \arg\min F(u) \tag{2}$$

3.3 Potential functions

The choice of the potential functions φ and ψ is supposed to lead us to the best solution which is determined by features of altimetric reconstruction in urban environment. Let us express some common-sense remarks about urban environment.

1. A lot of surfaces are horizontal (or about): streets, pavements, terraces, gardens and yards, etc.

2. Other surfaces are flat, but oblique, in particular the sides of the roofs.

3. Many discontinuities have to be found in the vertical ortho-photographic projection which we want to make of the city, the frontages in particular. Nevertheless, these surfaces can give measurements which do not correspond the real model because of the angle of scanning of the laser which can hit the frontages or cling on convex objects: balconies, canopies, etc.

4. Finally, a small number of objects do not correspond to any of these models. It happens for vegetation, vehicle surfaces of car parks where these vehicles are gathered in a very dense way.

A lot of studies have been done to determine potential functions for filtering images while recovering edges (Nikolova, 2000; Charbonnier et al., 1997; Bouman et al., 1993). Some potential functions are convex, some are not. They can be smooth or non-smooth at the origin. We limit our interest to four choices for potential functions. Each of them, except for total variation, has a parameter to tune (denoted by β).

Huber function (Figure 6(a)):

$$\varphi(t) = t^2 I(|t| < \beta) + (\beta^2 + 2\beta||t| - \beta|)I(|t| \geq \beta) \tag{3}$$

where I(p)=1 if p is true and I(p)=0 otherwise. This function is supposed to preserve slopes on the surface.

Total variation function (Figure 6(b)):

$$\varphi(t) = |t|. \tag{4}$$

Since this function is non-smooth at zero, it causes steplike zones on the surface (Nikolova, 2000).
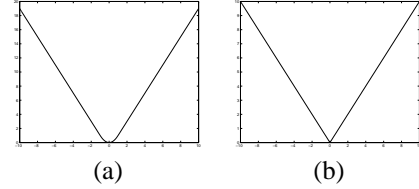

Figure 6: (a) Huber and (b) total variation function.

Generalized Gaussian function (Figure 7(a)):

$$\varphi(t) = |t|^\beta \quad 1 \leq \beta \leq 2. \tag{5}$$

Truncated quadratic function (Figure 7(b)):
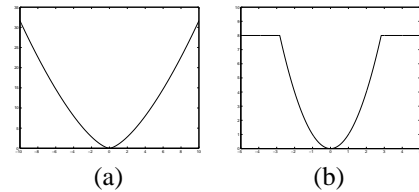
$$\varphi(t) = min\{t^2, \beta\}. \tag{6}$$

Figure 7: (a) generalized Gaussian and (b) truncated quadratic function.

3.4 Optimization algorithm

In order to find an optimum of the cost function several algorithms may be used (Li, 1995). Conjugated gradient is one of them. It is useful when the cost function is convex. Since not all the potential functions are convex in our case, we can use stochastic optimization methods. One of them is Iterated Conditional Modes (ICM) (Li, 1995) algorithm which has the following steps.

1. Initialization of the surface;

2. For each point

   - compute cost function values for all possible values the surface can have
   - attribute to the point the value which minimizes the cost function

3. Stop calculations if there are no changes at step 2; otherwise - come back to step 2.

ICM algorithm is a relatively fast optimization technique which unfortunately does not converge towards the global optimum unless initial point is close from it. Another very known technique is simulated annealing which gives a global optimum but is considerably more expensive in calculation time (Picard et al., 1995).

4 COMPARISON OF RESULTS

4.1 Methodology

Obviously, the quality of the results is not to be determined only visually. Correlation values with a ground truth can be used as quality measures in this case. The Digital Elevation Model (DEM), obtained from high resolution optical images, is taken as a reference here. A correlation coefficient is calculated between two vectors: a vector X of the DEM elevation values and a vector Y of the surface elevation values obtained with the laser scanner data:

$$r = \frac{\sum_{i=1}^{N} z_x z_y}{N - 1}$$

where

$$z_x = \frac{X - \bar{X}}{std(X)}, \quad and \quad z_y = \frac{Y - \bar{Y}}{std(Y)}$$

where $\bar{X}$, $\bar{Y}$ - mean values of the vectors X and Y respectively, $std(X)$, $std(Y)$ - their standard deviations, N - a number of elements in a vector, r - the correlation coefficient. A perfect correspondence between interpolated measurements and the DEM should lead us to a coefficient r equal to 1.

The resolution of the DEM is 10cm, and the resolution of a surface issued from laser is 1.80m. In order to compare our results to the reference, we perform the following steps. For each point of the resultant surface we find the corresponding point in the reference DEM. Then the value for comparison is taken as the median value of all the points inside the 5x5 window the reference DEM. There are some points where the reference DEM does not provide any information (Figure 8) (absence of textures on very uniform surfaces or hidden parts during the construction of the DEM). In the first case, the median value makes it possible to correct this absence, in the second (too large zones) the point is ignored in the correlation calculation.

We also noticed that the area of study contained 2 different zones: the largest part of the area contains mostly buildings, but the part of the area located at the top of the scene,

has vegetation with much more irregular geometry. Since this vegetation area may strongly influence the comparison, we evaluated our results with and without this zone.

Figure 8: The Digital Elevation Model used as a reference. The black values correspond to pixels where altitude values are not determined

4.2 Experimentation

To start, we choose both potential functions to be the same: $\psi = \varphi$. We initialized the optimization algorithm with different surfaces: white noise, results of triangle-based linear interpolation, results of nearest neighbour interpolation, results of kriging.

The density of primary laser data is about 1 point per 3.24 m^2. We selected the grid size to have the same density of points in the DSM: it corresponds to a sampling step of 1.8m.

The chosen method of optimization is the ICM for its more reduced calculating time. A significant parameter in this algorithm is the choice of the step in altitude (the height discretization). A too small step significantly increases the calculations since it is necessary to calculate the potential function for all these altitudes. A too coarse step leads to a too schematic description of the buildings but can also produce false minima. We chose a step of 50 cm, quite compatible with the required space resolution. For these initial surfaces, we obtained the results of correlation of Table 1.

At the initialisation, we can notice that kriging gives better results than the linear interpolation, the nearest neighbor interpolation is worse. We also can see that the zone of vegetation has tendency to degrade the correlation.

We take linear interpolation results as an initial surface, because they give the better output for $\alpha = 1$ (see Table 1). The results are presented on Figures 9 and 10. The horizontal line gives the correlation between the DEM and the best initialization surface (kriging for both figures) in order to see if the energy minimization approach outperforms the classical ones or not. A curve located below this line indicates that optimization degrades the initial solution.

	Initialisation		After optimization	
	1	2	1	2
White noise	0.0170	0.0177	0.9249	0.9395
Linear interpolation	0.9060	0.9311	0.9268	0.9402
Nearest neighbour interpolation	0.8627	0.8989	0.9254	0.9396
Kriging	0.9193	0.9406	0.9221	0.9201

Table 1: Correlation coefficients between the reference DEM and the calculated DSM at the initialisation (different interpolation methods are tested) and after energy minimization with the Huber function ($\alpha = 1, \beta = 1$). Results are evaluated with the vegetation area (column 1) or without (column 2).
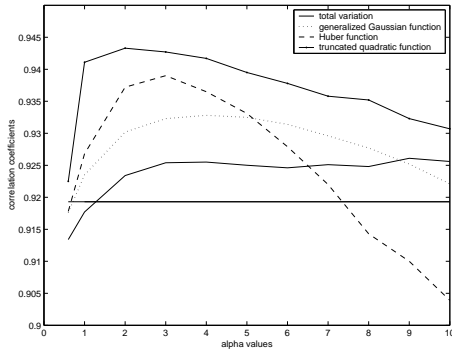

Figure 9: Search for an optimum for the area with vegetation

For the generalized Gaussian function we take $\beta = 1.2$, and for truncated quadratic function we take $\beta = 50$, because it gives better correlation results than other values of β. We can see the results for four potential functions, where truncated quadratic function gives the best result (for $\alpha = 2$), while total variation gives the worst result. The results of the evaluation without the zone of vegetation are presented on Figure 10. We notice that for a better initial value of correlation, it is difficult to improve it. In particular the total variation potential function always gives results lower than the initial solution, showing very clearly which the imposed solution (a solution by horizontal zones, without discrete slopes) is not in agreement with the DEM measured with stereo correlation.
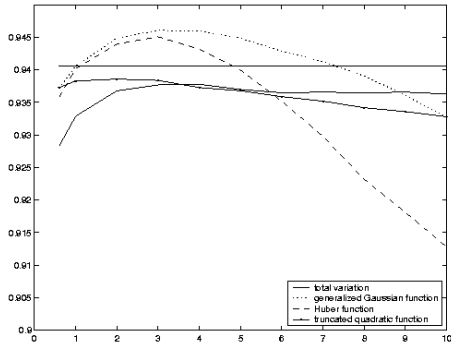

Figure 10: Search for an optimum for the area without vegetation

The best result for the area including the vegetation is shown on Figures 11 and 12.
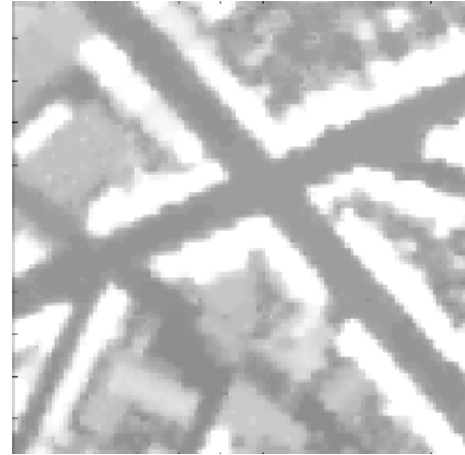

Figure 11: Potential functions are truncated quadratic functions and $\alpha = 2$
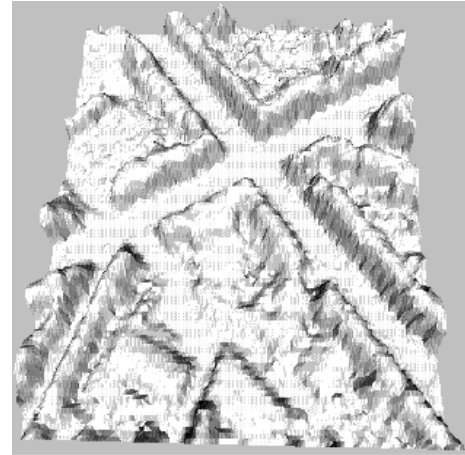

Figure 12: 3D representation of Figure 11

The best result without the vegetation part is on Figures 13 and 14, i.e. for getting these results we exclude the vegetation part (the upper part on the image) before calculating the correlation coefficient.

5 CONCLUSION

The choice of potential functions as well as their parameters obviously determine the quality of reconstruction. We chose the same potential functions for both terms of the energy. That seems to be logical but not necessary and we will check this point. One can imagine that the results could still be improved in two ways: by reducing the step of the grid of sampling (taken here equal to 1.8 m), by reducing the discretization of altitude (selected here to 0.5 m). Nevertheless, this progress is probably modest and will be paid by calculation time. A more interesting direction is probably to introduce these improvements gradually during the reconstruction: starting with coarse parameters, one refines them during optimization. This technique is connected with the multi-grid approaches of the numerical analysis.

Figure 13: Potential functions are generalized Gaussian functions and $\alpha = 3$

We notice that in all our results, a choice of a strong parameter of regularization (about 3) improves the quality criterion of correlation. We did not connect yet this value to precise physical sizes allowing to explain this result. One can see that in the equation of the potentials, the summations are made on very different numbers of points for the data-term (a number of terms depends on the local density of measurements) and for the term of regularization (a number fixed and chosen equal to 8). That seems logical since in the absence of measurement one wishes to have more regularized surfaces, while in the case of strong density of measurements, one will have confidence in the data (the regularization is thus adaptive according to the data). Nevertheless this weighting probably deserves a particular study because the law of adaptation is very empirical and can probably be improved.
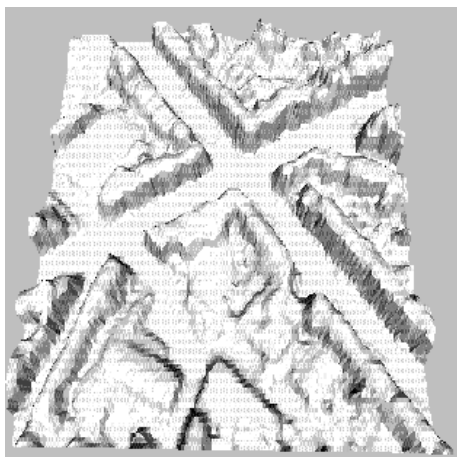

Figure 14: 3D representation of Figure 13

We also saw that the potential functions guided the reconstruction well towards theoretically foreseeable specific profiles. The model adopted today does not make it possible however to control locally the type of a solution. It would certainly be useful to be able to vary the criterion locally. Unfortunately, it will probably not be possible to guarantee an unspecified property (convergence, optimality, ad-

equacy with the model) of the solution thus obtained. It is however a direction which we wish to explore. Its difficulty lies of course in the choice of the criterion which makes it possible to decide about a type of reconstruction: without discontinuity, with discontinuity of the derivative, discontinuity of the function.

Finally we also notice that we seriously miss a good quality measure of the reconstruction. We adopted the criterion of correlation with the DEM model we have. First of all this DEM is not perfect and some details may have been filtered in the reference DEM which can exist in the laser profile. Then the correlation is not an irreproachable criterion. We also tested a least squares criterion between the two surfaces which should be equivalent for very close surfaces, but gave in fact results a little bit different from the ones of the correlation. A visual observation of the reconstructed images shows that the correlation prefers surfaces a little too smoothed whereas the human observer is less disturbed by local noises if the transitions are strictly respected.

REFERENCES

Behan, A., 2000. "On the matching accuracy of rasterised scanning laser altimeter data", *ISPRS Congress 2000*, Vol. XXXIII, Part B2, pp. 75-82, Amsterdam.

Bouman, C., Sauer, K., 1993. "A generalized Gaussian image model for edge-preserving MAP estimation", *IEEE Trans. on Image Processing*, vol. 2, issue 3, pp. 296-310.

Charbonnier, P., Blanc-Féraud, L., Aubert, G., Barlaud, M., 1997. "Deterministic edge-preserving regularization in computed imaging", *IEEE Trans. on Image Processing*, vol. 6, No. 2, pp. 298-311.

Geman, D. and Reynolds, G., 1992. "Constrained Restoration and the Recovery of Discontinuities" *IEEE Trans. Pattern Anal. Machine Intell.*, vol.14, pp. 367-383.

Li, S., 1995. *"Markov Random Field Modeling in Computer Vision"*, Springer Verlag.

Lohmann, P. and Koch, A., 1999. "Quality assessment of laser-scanner-data", *ISPRS Workshopp on Sensing and Mapping from Space*, University of Hanover, on CD-ROM.

Nikolova, M., 2000. "Local strong homogeneity of a regularized estimator", *SIAM J. Appl. Math*, vol. 61, No. 2, pp. 633-658.

Noel, A., 1991. *"Statistics for spatial data"*, A Wiley-Interscience publication.

Picard, R. and Pentland, A., 1995. "Temperature and Gibbs image modeling" Media Laboratory, Perceptual Computing 254, MIT, Cambridge, MA.

Watson, D., 1992. *"Contouring: a guide to the analysis and display of spatial data"*, Pergamon Press.